

T1-1-a-1

Ambient Vibration Tests and Modal Identification of Structures by FDD and 2DOF-RD Technique

Yukio TAMURA¹, Lingmi ZHANG², Akihito YOSHIDA³,
Shinji NAKATA⁴ and Takayoshi ITOH⁵

^{1 and 3}Tokyo Institute of Polytechnics, Kanagawa 243-0297, JAPAN

E-mail: yukio@arch.t-kougei.ac.jp and yoshida@arch.t-kougei.ac.jp

²Nanjing University of Aeronautics & Astronautics, Nanjing, CHINA

E-mail: lmzae@nuaa.edu.cn

⁴Asahikasei Corporation, Tokyo 160-8345, JAPAN

⁵Tokyo Electric Power Services, Tokyo 100-0011, JAPAN



ABSTRACT:

The dynamic characteristics of structures are evaluated rather frequently by measuring their vibrations. This is done to investigate wind vibrations of high-rise buildings or for other purposes. However, few vibration evaluations have focused on changes in the structural properties of buildings or on the rigidity of main structures and non-structural walls during construction. This paper describes changes of the dynamic characteristics of a 15-story office building in four construction stages from the foundation stage to completion. The structural properties of each construction stage were modeled as accurately as possible by FEM, and evaluation of the stiffness of main structural frame and comparing these FEM results with measurement results performed non-load-bearing elements. Full-scale measurements were also carried out on high-rise chimney, and good correspondence was shown with vibration characteristics obtained by the 2DOF-RD technique and the Frequency Domain Decomposition method.

1. Introduction

Dynamic characterization of civil engineering structures is becoming increasingly important for dynamic response prediction, finite element modal updating and structural health monitoring, as well as for passive and active vibration control of buildings, towers, long-span bridges, etc. The dynamic characteristics of a structure can be obtained by traditional experimental modal analysis. This requires artificial excitation and measurement of both responses and excitation forces. Many civil engineering structures can be adequately excited by ambient (natural) excitations such as wind, turbulence, traffic, and/or micro-seismic tremors. Ambient modal analysis based on response measurements has two major advantages compared to traditional analysis. One is that no expensive and heavy excitation devices are required. The other is that all (or part) of the measurements can be used as references, and multi-input multi-output techniques can be used for modal analysis, thus enabling easy handling of closely-spaced and even repeated modes.

This paper introduces a research project launched for experimental modeling of a newly designed and constructed 15-story office building by ambient modal analysis. Ambient response measurements of the CFT building in the field at different construction stages were planned in order to investigate the variation of its dynamic characteristics during construction. This was done in order to examine the separate contributions of the steel frames, the column concrete, the floor slabs, the external walls, the internal walls, etc., to the building's dynamic characteristics. Detecting the change in the dynamic characteristics with the addition of structural members or architectural parts enabled more accurate quantitative evaluation of the

contribution of these members and parts to the analytical finite element model (FEM) of the building. Another research project on ambient response field measurements of high-rise steel chimney is also reported, where the dynamic characteristics are obtained by frequency domain decomposition (FDD) and a newly proposed 2DOF-RD technique.

2. Dynamic Characteristics of 15-Story Office Building^{[1][2]}

2.1 Tested CFT Building

The building tested is a middle-rise 15-story office building 53.4 m high, located in Ichigaya, Tokyo. It extends from 6.1m underground to 59.15m above basement level, as shown in Figure 1. It has one story beneath ground level and 15 stories above. The columns are concrete-filled-tube (CFT), as shown in Figure 2, and the beams are wide-flange steel. The floor comprises a concrete slab and steel deck. The exterior walls of the first floor are of pre-cast concrete. The walls from the second floor to the top are of autoclaved lightweight concrete (ALC). The ALC exterior walls are attached by a half locking method. The interior walls are attached by the slide method. The plan of a standard story is 22.2m long by 13.8m wide, and the floor-to-floor height is 3.8m. The piles are under the foundations, and the underground story are of SRC (steel-encased reinforced concrete). When the steel frame portion was erected up to the 11th floor, the CFT columns were filled with concrete. The concrete was placed by the pressing method from the first floor pedestal portion. After that, the steel frame was erected up to the 15th floor, and the floor slab concrete was placed after the concrete was placed in the CFT columns. The concrete strengths were 24N/mm^2 underground, 42N/mm^2 for the column filling, and 21N/mm^2 (lightweight concrete) above ground.

2.2 Field Measurement

Field ambient response measurements were conducted at four different construction stages. Figure 3 shows the transition of construction stages. Stages I and II measurements were conducted to compare the dynamic properties before and after concrete filling of the CFT columns up to the 11th floor. At this point, the floor slab concrete for each story had not yet been placed. Stage III was when the main structure of the building was completed. Concrete filling of CFT columns and slab concrete placing of each story were finished, and the dynamic properties of the main structure itself were checked. A tower crane was installed from Stage I to Stage III. Stage IV was at completion of the building, and the influence of non-load-bearing walls was checked. Servo-type accelerometers were used for ambient response measurement. With high sensitivity and resolution (10^{-6} V/g), a sufficient response signal was obtained. The sampling rate was set at 20 Hz, with a Nyquist frequency of 10 Hz. The duration of each record was 1,800 seconds.

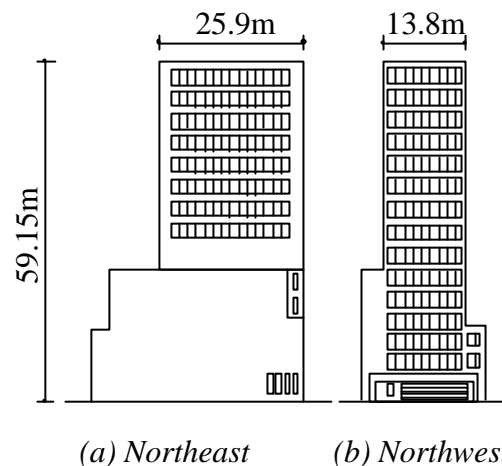


Fig. 1 Elevation of 15-story office building

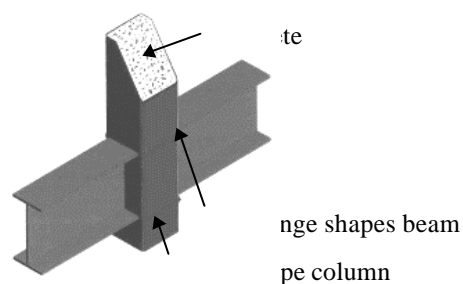


Fig.2 Concrete-Filled-Tube (CFT) column

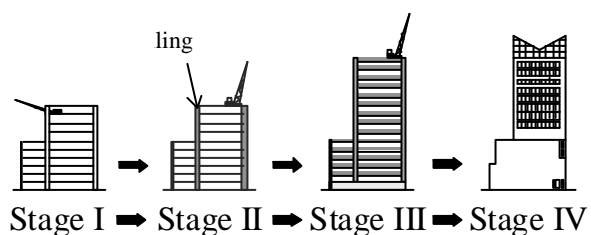


Fig.3 Transition of construction stage

The time series of each channel had 36,000 points. Full ambient response measurements of the CFT building took less than 6 hours to finish within the same day. At Stages I, II and III, eight accelerometers were installed at the top of the CFT building, and six accelerometers were installed below ground level.

At Stage IV, fourteen accelerometers were used for one setup with two accelerometers at the 15th floor as references. It is reasonably assumed that the floor was subject to lateral rigid body motion. The measured vibration was translated into equivalent motions at the desired corners. Accelerometers excluding reference accelerometers were used as roving sensors for the 1st, 2nd, 3rd and 4th setups. Three accelerometers were typically placed in the southeast (x direction) and northeast corners (x and y directions) from the 7th floor to 15th floor as well as in the roof. Six accelerometers were placed at the 2nd, 4th and 6th floors, respectively.

The ambient data recorded during the field measurement was processed in the frequency domain afterwards. Power spectral density was estimated using full measurement data with a frame of 1024 data points. 512 spectrum lines, with frequency resolution of 0.01953 Hz, were calculated. A Hanning window was applied as usual with 66.7 % overlap to increase the average number.

2.3 System Identification with Frequency Domain Decomposition

2.3.1 Modal Frequency & Mode Shape Identification

Instead of using PSD directly, as it does by the classical frequency domain technique, the PSD matrix is decomposed at each frequency line via Singular Value Decomposition (SVD). SVD has a powerful property of separating noisy data from disturbance caused by unmodeled dynamics and measurement noise. For the analysis, the Singular Value plot, as functions of frequencies, calculated from SVD can be used to determine modal frequencies and mode shapes.

It has been proved [3] that the peaks of a singular value plot indicate the existence of structural modes. The singular vector corresponding to the local maximum singular value is unscaled mode shape. This is exactly true if the excitation process in the vicinity of the modal frequency is white noise. One of the major advantages of the FDD technique is that closely-spaced modes, even repeated modes, can be dealt with without any difficulty. The only approximation is that orthogonality of the mode shapes is assumed. Figure 4 presents the SV Plots of the CFT building at

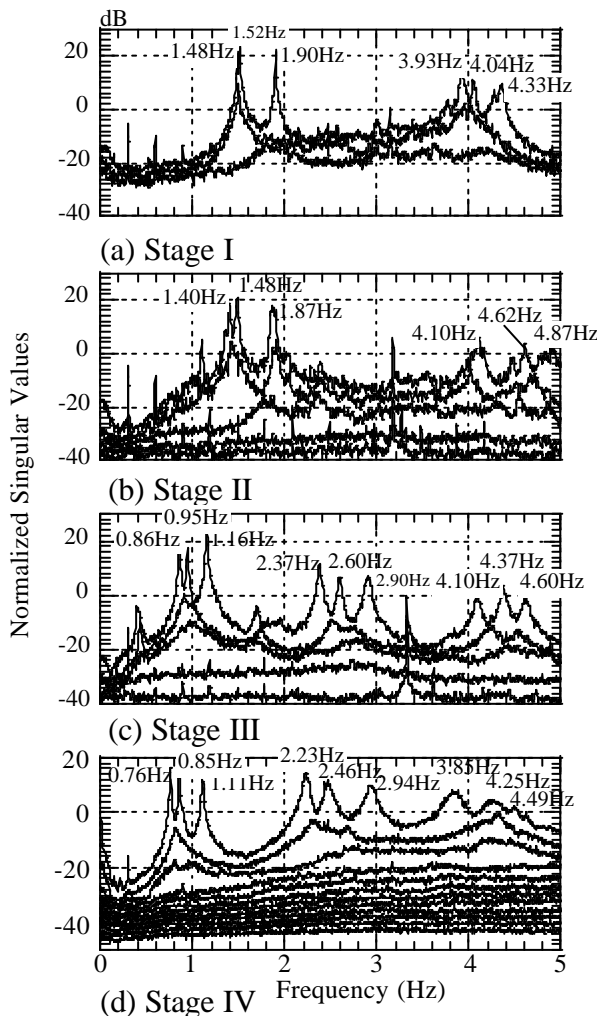


Fig.4 Singular value plot at the CFT building

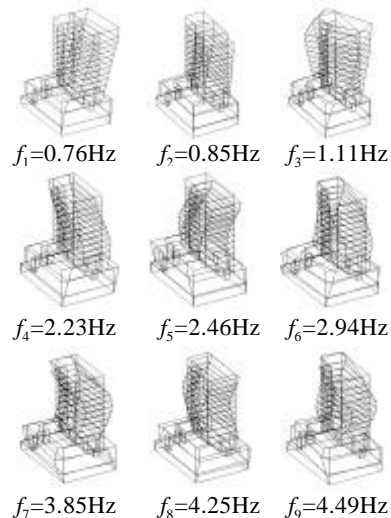


Fig.5 Mode shape of the CFT Building at Stage IV

different stages.

Table 1 gives nine identified modal frequencies. Figure 5 depicts the corresponding nine mode shapes. In the FDD technique, the PSD matrix is formed first from ambient response measurements. ARTEMIS was used as the analysis software.

2.3.2 Modal Damping Estimation

One of the major objectives of the research project was to estimate the modal damping of the CFT building. The basic idea of the FDD method is as follows [4]. The singular value in the vicinity of natural frequency is equivalent to the power PSD function of the corresponding mode (as a SDOF system). This PSD function is identified around the peak by comparing the mode shape estimate with the singular vectors for the frequency lines around the peak. As long as a singular vector is found that has a high Modal Amplitude Coherence (MAC) value with the mode shape, the corresponding singular value belongs to the SDOF function. If at a certain line

none of the singular values has a singular vector with a MAC value larger than a certain limit value, the search for matching parts of the PSD function is terminated. Figure 6 gives a typical “bell” of the SDOF system—the first and second modes of the CFT building. The remaining spectral points (the unidentified part of the PSD) are set to zero. From the fully or partially identified SDOF spectral density function, the natural frequency and the damping ratio can be estimated by taking the PSD function back to the time domain by inverse FFT as a correlation function of the SDOF system, as shown in Figure 7. From the free decay function, the natural frequency and the damping are found by the logarithmic decrement technique. In the FDD, the power spectral density functions should be estimated via discrete Fourier transform (DFT) before the SVD. It is well known that leakage error in PSD estimation always takes place due to data truncation of DFT. Leakage is a kind of bias error, which cannot be eliminated by windowing, e.g. by applying a Hanning window, and is harmful to the damping estimation

Table 1 Natural frequency of CFT building

Mode	Natural Frequency (Hz)			
	Stage II	Stage III	Stage IV	Stage V
1 st	1.48	1.40	0.86	0.76
2 nd	1.52	1.48	0.95	0.86
3 rd	1.90	1.87	1.16	1.11
4 th	3.93	4.10	2.37	2.23
5 th	4.04	4.62	2.60	2.47
6 th	4.33	4.87	2.90	2.94
7 th	-	-	4.10	3.85
8 th	-	-	4.37	4.26
9 th	-	-	4.60	4.47

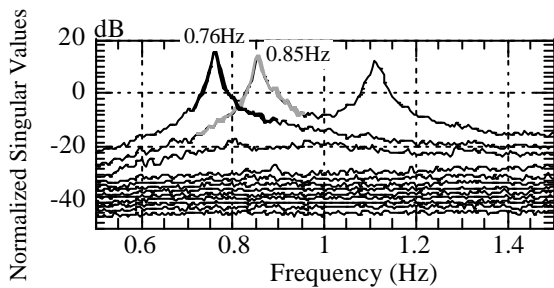


Fig.6 Singular value plot of the CFT building at Stage IV (Frequency ranges 0.5-1.5Hz)

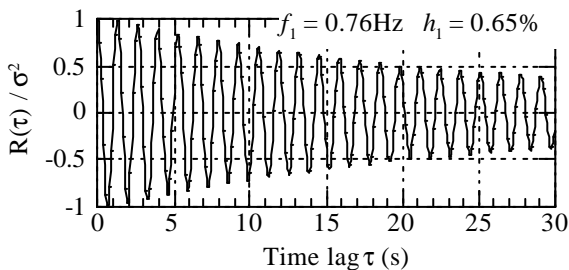


Fig.7 Correlation function of the 1st mode at Stage IV

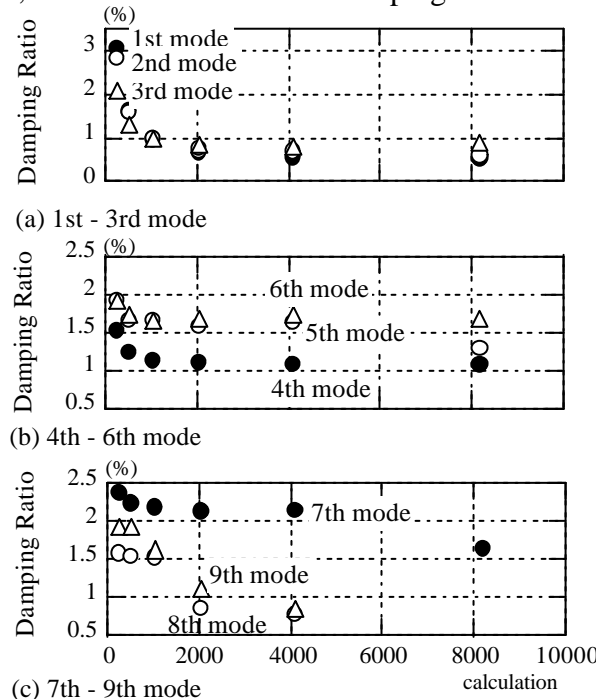


Fig.8 Changes of damping ratio vs. data points at Stage IV

accuracy, which relies on the PSD measurements.

The bias error caused by leakage is proportional to the square of the frequency resolution^[5]. Therefore, increasing frequency resolution is a very effective way to reduce leakage error. Thanks to the volume of data taken at field response measurements, we can afford to use more data, i.e. increase frequency resolution, in PSD computation. In order to show the influence of the frequency resolution on the damping estimation accuracy, 256, 512, 1024, 2048 and 4096 data points

were used to calculate the PSD functions. The corresponding frequency resolutions were 0.0783, 0.0392, 0.0195, 0.00977 and 0.00488 Hz, respectively. Figure 8 presents the changes of the damping ratios with the number of data points used for PSD calculation at Stage IV. It is very interesting to observe that, as predicted by the theory of random data procession, the damping ratios of all modes decrease, while the number of data points, or frequency resolution, increase. It appears that damping estimates converge when the number of data points is large enough (reach to 4096 or 8192). Table 2 shows the damping ratios of all construction stage with enough data points to be used for PSD calculation.

Table 2 Damping Ratio of CFT building

Mode	Damping Ratio (%)			
	Stage I	Stage II	Stage III	Stage IV
1 st	0.27	0.75	0.53	0.65
2 nd	0.32	0.70	0.65	0.74
3 rd	0.18	0.80	0.59	0.84
4 th	0.53	0.81	0.61	1.10
5 th	0.40	0.60	0.72	1.56
6 th	0.99	1.25	0.84	1.67
7 th	-	-	0.86	2.12
8 th	-	-	0.76	0.85
9 th	-	-	0.79	1.11

2.4 Modal Identification by FEM Analysis

2.4.1 FEM Model

The FEM models were based on the design documents. For the model before filling concrete in the CFT columns, as Stage I, the columns were of steel pipe and the CFT columns were of steel pipe portions, and the columns, which compounded the concrete, as Stage II. For the model up to the 11th floor (Stages I and II), two cases were compared: the pedestal assumed as pinned, and the pedestal assumed as fixed. After the 15th floor of the building was completed and the slab concrete was placed, as Stage III, the field measurement results were compared for the model with steel floor beams and that with composite beams. The assumption of a synthetic beam was taken as the form where 1/10 of the length of the beam was derived from Design Recommendations for Composite Constructions^[6]. The underground portion was modeled as CFT columns and RC walls. The RC walls of the underground portion were modeled as shell elements. Moreover, the analysis model upon building completion, as Stage IV, considered two cases: the stiffness of the main structure only, and the stiffness of the main structure as well as the stiffness of the exterior walls. The non-load-bearing curtain walls were modeled as spring elements, and the stiffness was determined so that the first mode natural frequency from the field measurement agreed with the FEM value. The general-purpose structural analysis program SAP-2000 was used as the analysis software.

2.4.2 FEM Results

The vibration modes obtained by FEM analysis at building completion (Stage IV) are shown in Table. 3. In the FEM analysis, the building's stiffness was estimated only for the members of the main structure. As a result, the FEM results are evaluated slightly smaller than the actual values. The stiffness of the building's exterior walls was therefore added so that the first vibration mode was nearly identical to the actual value. As a result, satisfactory agreement was obtained up to the sixth vibration mode. The stiffness of the walls at this stage was 9.8 kN/cm/m. This is reported in a paper that describes a survey investigation on the stiffness of ALC outer walls^[7]. The stiffness used for this analysis is almost the same as in this paper.

The lowest natural frequency for Stage IV (at building completion) was measured as 0.76Hz, where Y-dir. translational motion is predominant. Survey investigations of the natural period

of multi-story buildings in Japan^[8] show that the lowest natural frequency f_1 (Hz) of a building with a height H (m) is approximated by the following expression.

$$\begin{cases} f_1 = \frac{H}{0.020} & \text{(Steel structures)}^{[8]} \\ f_1 = \frac{H}{0.015} & \text{(Steel encased reinforced concrete structures)}^{[8]} \end{cases}$$

The height of this building is 59.15m. Thus, the frequency derived from this formula for steel structures is 0.85Hz, and that for steel encased reinforced structures is 1.13Hz. These results show that the natural frequencies of this building are close to those for steel structures.

Table 3 Nine mode shapes and their natural frequencies of a CFT building obtained by FEM analysis and FDD (Stage IV)

Mode									
Frequency(Hz)	f_1	f_2	f_3	f_4	f_5	f_6	f_7	f_8	f_9
FEM	0.74	0.82	1.02	1.92	2.18	2.45	-	-	-
Tuned FEM	0.76	0.87	1.15	2.14	2.53	3.02	3.85	4.26	4.67
FDD	0.76	0.86	1.11	2.23	2.47	2.94	3.85	4.26	4.47

3. Dynamic Characteristics of a Chimney^{[9][10]}

3.1 Field Measurement Set-up

Ambient response measurements of a 230m-high chimney were conducted to investigate its dynamic characteristics. Figure 9 shows the elevation and plan of the tested chimney, consisting of steel trusses and a concrete funnel. The chimney has an octagonal cross section. Accelerometers were installed on three different levels, as shown in Fig.10. Two horizontal components (x, y) and one vertical component (z) were measured at each level. A sonic anemometer was also installed at the top of the chimney. The sampling rate of the acceleration records was set at 100Hz, and the ambient responses were measured for 90 minutes in total.

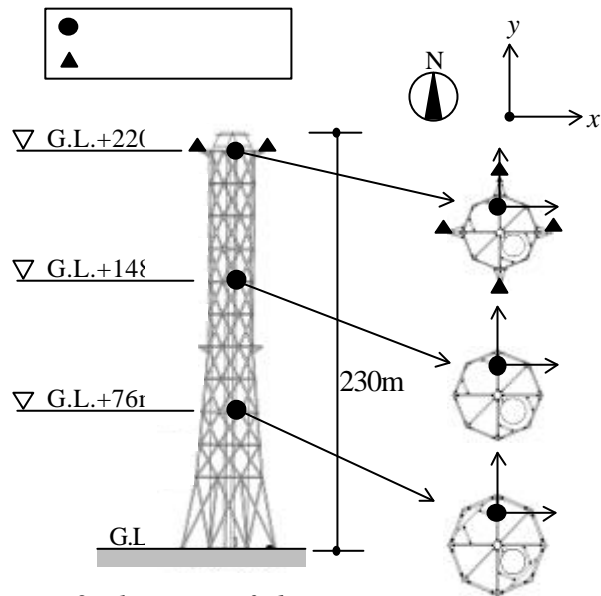


Fig.9 Elevation of chimney

3.2 System Identification by 2DOF-RD technique and FDD

3.2.1 Dynamic characteristics of chimney estimated by 2DOF-RD technique

Figure 10 shows the power spectrum density functions of accelerations at three different heights. Peaks corresponding to several natural frequencies are clearly.

At first, the general Random Decrement (RD) technique assuming a SDOF system was applied for system identification using the ambient y -dir. acceleration records at the top level, GL+220m. By processing with a numerical band-pass filter with a frequency range of 0.06Hz - 1.0Hz, only the frequency components around the lowest peak near 0.40Hz depicted in Fig.10 were extracted. The initial amplitude of the acceleration to get the Random Decrement

signature (RD-signature) was set at the standard deviation, \mathbf{s}_{acc} . Figure 11 shows the obtained RD-signature, where a beating phenomenon is clearly observed, suggesting two closely located predominant frequency components. By carefully studying the peak near 0.4Hz, it is seen that there are actually two peaks: at 0.40Hz and 0.41Hz. These peaks are named f_1 and f_2 , respectively, in this paper. The general RD technique assuming a SDOF system can efficiently evaluate the damping ratio and the natural frequency only for a well-separated vibration mode, but not for the above case. In order to evaluate the two closely located two vibration modes, the 2DOF-RD technique is proposed, where the superimposition of the two SDOF systems with different dynamic characteristics is made. The RD signature shown in Fig.11 was approximated by superimposition of the two different damped free oscillations as follows:

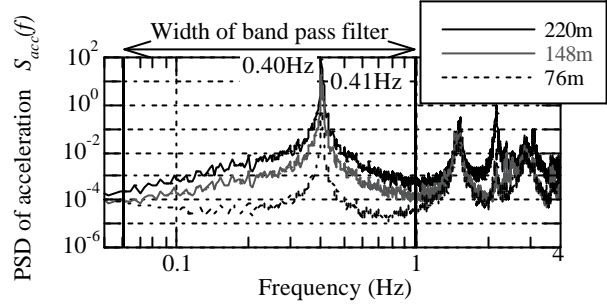


Fig.10 Power spectrum of tip acceleration (Y-dir)

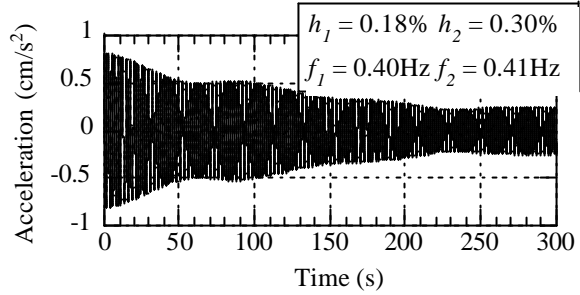


Fig. 11 RD signature of tip acceleration (Y-dir.)

$$R_i(t) = \frac{x_{0i}}{\sqrt{1-h_i^2}} e^{-h_i \omega_i t} \cos\left(\sqrt{1-h_i^2} \omega_i t - \mathbf{f}_i\right)$$

$$R(t) = \sum_{i=1}^2 R_i(t) + m$$

where $R(t)$: RD signature, $R_i(t)$: i -th mode component ($i = 1$ and 2), x_{0i} : initial value of i -th mode component, h_i : i -th mode damping ratio, ω_i : i -th mode circular frequency, t : time, \mathbf{f}_i : phase shift, and m : mean value correction of RD signature.

The approximation was made by the least-square method, and the damping ratio and the natural frequency of the chimney were estimated at 0.18% and 0.40Hz for the 1st mode, and 0.30% and 0.41Hz for the 2nd mode. The dynamic characteristics of the 3rd and 4th modes were also estimated by the 2DOF-RD technique.

3.2.2 Dynamic characteristics of chimney estimated by FDD

The FDD method was applied to the six horizontal components of the acceleration responses at the three different heights to evaluate the chimney's dynamic characteristics. Figure 12 shows the frequency distribution of the singular value obtained by the FDD method. Figure 13 is a close-up in the range of 0.1Hz - 0.7Hz, where the upper line shows two peaks at 0.40Hz and 0.41Hz, corresponding to f_1 and f_2 in 3.2.1. The lower line has a peak between 0.40Hz and 0.41Hz, and the right-side slope can be connected to the first peak of the upper line, and the left to the second peak. This forms a "bell" as already shown in Fig.6, so the combination of the upper and lower lines can closely identify the located modes.

Fig. 14 shows the auto-correlation function of the 1st mode obtained by the inverse FFT for the separated peak as above. Figure 15 shows the variations of the damping ratios of the lowest two modes with the number of data points used for PSD calculation. The damping ratios converge to precise values with increase in the number of data points.

Table 3 shows the dynamic characteristics of the chimney obtained by the FDD method with enough PSD data points and by the RD technique, where the 2DOF-RD technique was used for the 1st, 2nd, 3rd and 4th modes. These results show fairly good agreement between the FDD and 2DOF-RD techniques, except for the 3rd-mode damping ratio.

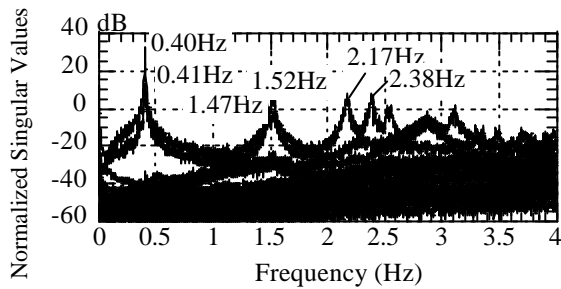


Fig. 12 Frequency distribution of singular value

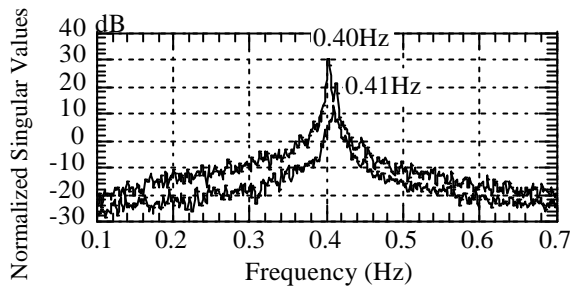
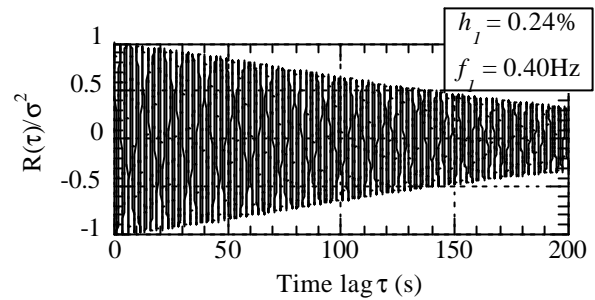
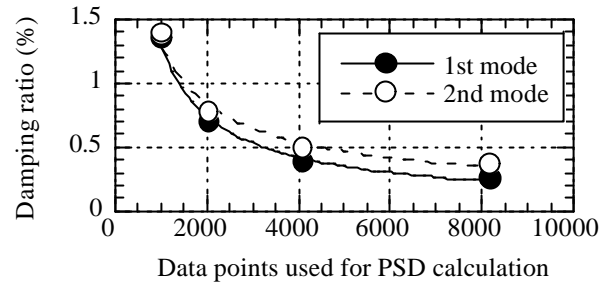
Fig. 13 Frequency distribution of singular value
(Close-up: frequency range 0.1-0.7Hz)

Fig. 14 Correlation function obtained by FDD

Fig. 15 Variations of damping ratio with
PSD data points

4. Concluding Remarks

The dynamic characteristics of two actual structures were estimated by the FDD and 2DOF RD techniques using their ambient responses, and also by FEM. The results were all satisfactory and agreed well.

Table 3 Dynamic characteristics of chimney

Mode	Natural Frequency(Hz)		Damping Ratio(%)	
	RD	FDD	RD	FDD
1 st	0.40	0.40	0.18	0.24
2 nd	0.41	0.41	0.30	0.39
3 rd	1.47	1.47	0.83	0.3
4 th	1.53	1.52	0.85	0.91
5 th	2.17	2.17	0.55	0.65
6 th	2.38	2.38	0.42	0.39
7 th	-	2.87	-	-
8 th	-	3.10	-	0.77

References

- [1] Tamura, Y., Zhang, L., Yoshida, A., Cho, K., Nakata, S., and Naito, S., Ambient vibration testing & modal identification of an office building with CFT columns, 20th International Modal Analysis Conference, pp141-146, 2002
- [2] Miwa, m., Nakata, S., Tamura, Y., Fukushima, Y., and Otsuki, T., Modal identification by FEM analysis of a building with CFT columns, 20th International Modal Analysis Conference, 2002
- [3] Ibrahim, S.R. and Mikulcik, E.C., A Method for the Direct Identification of Vibration Parameters from the Free Response, Shock and Vibration Bulletin, 183-198, No. 47, Pt. 4, Sept. 1977
- [4] Brincker, R., Ventura, C.E. and P. Andersen, Damping Estimation by Frequency Domain Decomposition, Proc. of the 19th IMAC, 698-703, Feb. 2001
- [5] Bendat, J. and Piersol, A., <Random Data, Analysis and Measurement Procedures>, John Wiley & Son, New York, USA, 1986
- [6] Architectural Institute of Japan, Design Recommendations for Composite Constructions, 1985 (in Japanese)
- [7] Fukuwa, N., Nishizaka, R., Yagi, S., Tanaka, K, and Tamura, Y., Field measurement of damping and natural frequency of an actual steel-framed building over a wide range of amplitude, Journal of Wind Engineering and Industrial Aerodynamics, Vol.59, pp.325-347,1996.
- [8] Architectural Institute of Japan, Damping of Structures, 2000 (in Japanese)
- [9] Masuda, K., Sasajima, K., Yoshida, A. and Tamura, Y., Dynamic characteristics of a tall steel chimney. Part 1 Ambient response measurements, Summaries of Technical Papers of Annual Meeting, Architectural Institute of Japan, B-1, 2002 (in Japanese)
- [10] Yoshida, A., Tamura, Y., Masuda, K. and Ito, T., Dynamic characteristics of a tall steel chimney. Part 2 Evaluation of dynamic characteristics by 2DOF-RD technique and FDD, Summaries of Technical Papers of Annual Meeting, Architectural Institute of Japan, B-1, 2002 (in Japanese)